

Article

Binding of Distamycin A to UV-Damaged DNA

Aki Inase, Takashi S. Kodama, Jafar Sharif, Yan Xu, Hirohito Ayame, Hiroshi Sugiyama, and Shigenori Iwai

J. Am. Chem. Soc., **2004**, 126 (35), 11017-11023 • DOI: 10.1021/ja048851k • Publication Date (Web): 14 August 2004

Downloaded from <http://pubs.acs.org> on April 1, 2009

More About This Article

Additional resources and features associated with this article are available within the HTML version:

- Supporting Information
- Access to high resolution figures
- Links to articles and content related to this article
- Copyright permission to reproduce figures and/or text from this article

[View the Full Text HTML](#)



ACS Publications
High quality. High impact.

Binding of Distamycin A to UV-Damaged DNA

Aki Inase,[†] Takashi S. Kodama,[‡] Jafar Sharif,[§] Yan Xu,^{||} Hirohito Ayame,^{||}
Hiroshi Sugiyama,^{||,⊥} and Shigenori Iwai^{*,†,§}

Contribution from the Division of Chemistry, Graduate School of Engineering Science, Osaka University, 1-3 Machikaneyama, Toyonaka, Osaka 560-8531, Japan, Japan Biological Information Research Center (JBIRC), Japan Biological Informatics Consortium (JBIC), 2-41-6 Aomi, Koto-ku, Tokyo 135-0064, Japan, and Biomolecular Engineering Research Institute, 6-2-3 Furuedai, Suita, Osaka 565-0874, Japan, Department of Chemistry and Biotechnology, School of Engineering, The University of Tokyo, 7-3-1 Hongo, Bunkyo-ku, Tokyo 113-8656, Japan, Division of Biofunctional Molecules, Institute of Biomaterials and Bioengineering, Tokyo Medical and Dental University, 2-3-10 Kanda-Surugadai, Chiyoda-ku, Tokyo 101-0062, Japan, and Department of Chemistry, Graduate School of Science, Kyoto University, Kitashirakawa Oiwakecho, Sakyo-ku, Kyoto 606-8502, Japan

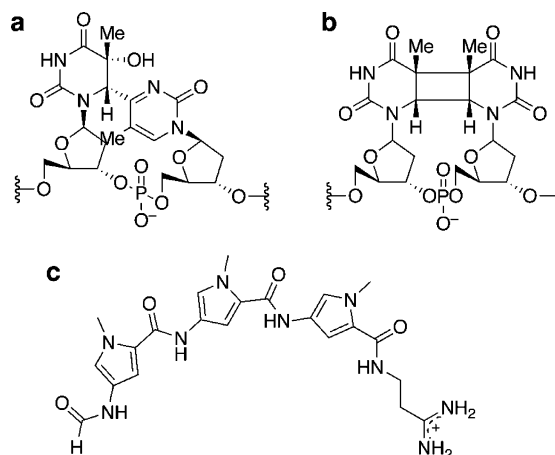
Received March 1, 2004; E-mail: iwai@chem.es.osaka-u.ac.jp

Abstract: We have found that distamycin A can bind to DNA duplexes containing the (6–4) photoproduct, one of the major UV lesions in DNA, despite the changes, caused by photoproduct formation, in both the chemical structure of the base moiety and the local tertiary structure of the helix. A 20-mer duplex containing the target site, AATT·AATT, was designed, and then one of the TT sequences was changed to the (6–4) photoproduct. Distamycin binding to the photoproduct-containing duplex was detected by CD spectroscopy, whereas specific binding did not occur when the TT site was changed to a cyclobutane pyrimidine dimer, another type of UV lesion. Distamycin binding was analyzed in detail using 14-mer duplexes. Curve fitting of the CD titration data and induced CD difference spectra revealed that the binding stoichiometry changed from 1:1 to 2:1 with photoproduct formation. Melting curves of the drug–DNA complexes also supported this stoichiometry.

Introduction

Ultraviolet (UV) light induces several types of base damage in DNA.¹ Among them, the *cis-syn* cyclobutane pyrimidine dimer (CPD) and the pyrimidine(6–4)pyrimidone photoproduct ((6–4) photoproduct), formed at adjacent pyrimidine bases, are the major UV lesions (Chart 1, a and b). Both of these photoproducts arise from a [2+2] cycloaddition, by direct absorption of UVB and UVC photons or by photosensitized triplet energy transfer of UVA photons,² but their biological properties are different. The (6–4) photoproduct is more mutagenic than the CPD,^{3–5} and, although human DNA polymerase η can correctly replicate DNA containing the CPD,^{6–8} efficient translesion synthesis past the (6–4) photoproduct has

Chart 1. Structures of the (6–4) Photoproduct (a), CPD (b), and Distamycin A (c)



not been found. To maintain genetic integrity, the (6–4) photoproduct must be removed by the nucleotide excision repair pathway in cells.^{9–11}

[†] Osaka University.

[‡] JBIC and Biomolecular Engineering Research Institute.

[§] The University of Tokyo.

^{||} Tokyo Medical and Dental University.

[⊥] Kyoto University.

(1) Ravanat, J.-L.; Douki, T.; Cadet, J. *J. Photochem. Photobiol., B* **2001**, *63*, 88–102.

(2) Douki, T.; Reynaud-Angelin, A.; Cadet, J.; Sage, E. *Biochemistry* **2003**, *42*, 9221–9226.

(3) LeClerc, J. E.; Borden, A.; Lawrence, C. W. *Proc. Natl. Acad. Sci. U.S.A.* **1991**, *88*, 9685–9689.

(4) Smith, C. A.; Wang, M.; Jiang, N.; Che, L.; Zhao, X.; Taylor, J.-S. *Biochemistry* **1996**, *35*, 4146–4154.

(5) Kamiya, H.; Iwai, S.; Kasai, H. *Nucleic Acids Res.* **1998**, *26*, 2611–2617.

(6) Masutani, C.; Araki, M.; Yamada, A.; Kusumoto, R.; Nogimori, T.; Maekawa, T.; Iwai, S.; Hanaoka, F. *EMBO J.* **1999**, *18*, 3491–3501.

(7) Masutani, C.; Kusumoto, R.; Yamada, A.; Dohmae, N.; Yokoi, M.; Yuasa, M.; Araki, M.; Iwai, S.; Takio, K.; Hanaoka, F. *Nature* **1999**, *399*, 700–704.

(8) Masutani, C.; Kusumoto, R.; Iwai, S.; Hanaoka, F. *EMBO J.* **2000**, *19*, 3100–3109.

(9) Wood, R. D. *J. Biol. Chem.* **1997**, *272*, 23465–23468.

We have been studying the molecular recognition of the (6–4) photoproduct (Chart 1a), using chemically synthesized oligonucleotides.¹² Our search for a protein that binds the (6–4) photoproduct-containing DNA revealed that the UV-damaged DNA-binding (UV-DDB) protein was the major factor for the recognition of this lesion in human cells.^{13,14} In the complex between the UV-DDB protein and the damaged DNA, the DNA helix was kinked at the damage site by an angle of about 55°. Although an NMR study suggested a solution structure of the (6–4) photoproduct-containing DNA with an overall helix bending of 44°,¹⁵ our previous study using fluorescence resonance energy transfer,¹⁶ in agreement with a molecular dynamics analysis,¹⁷ revealed that the DNA is not bent in the absence of protein binding. These results and other unpublished data strongly suggest that the DNA helix containing the (6–4) photoproduct can be kinked easily, and that the UV-DDB protein recognizes this aspect of the damaged DNA.

The UV-DDB protein is a heterodimer composed of the p127 and p48 subunits, and our attempts to produce this protein by the expression of its cDNA in bacteria or yeast were not successful. Recently, each subunit was reportedly produced in a baculovirus-insect cell system,¹⁸ but the amounts obtained by this method are limited. The heterodimeric structure, composed of relatively large subunits, complicates analyses of the functions of this protein and restricts its usage in application studies. Therefore, we started to seek a low-molecular-weight compound that recognizes UV damaged DNA. Some of the candidates were minor groove binders, such as netropsin, distamycin, and Hoechst 33258, which recognize the minor groove of AT-rich regions by van der Waals contacts and hydrogen bonds.^{19,20} In many crystal structures of protein–DNA complexes, especially in the cases of base excision repair enzymes, the general conformational change in the DNA caused by complex formation is a sharp kink of the helical axis toward the major groove at the protein binding site.^{21–25} Therefore, we expected that the minor groove binders might be able to bind to (6–4) photoproduct-containing DNA, which has the potential to be kinked easily, by an induced-fit mechanism similar to that suggested for the UV-DDB protein.

We now report that distamycin A (Chart 1c) can bind to DNA duplexes containing the (6–4) photoproduct, although photo-

Chart 2. Oligonucleotide Duplexes Used in This Study

TT-20	5'- CCTACGCGAATTCGGCATCC -3' 3'- GGATGCGCTTAAGCCGTAGG -5'
(6–4)-20	5'- CCTACGCGAA(6–4)CGGCATCC -3' 3'- GGATGCGCTTAAGCCGTAGG -5'
CPD-20	5'- CCTACGCGAA ^{CPD} CGGCATCC -3' 3'- GGATGCGCTTAAGCCGTAGG -5'
CC-20	5'- CCTACGCGAACCCGGCATCC -3' 3'- GGATGCGCTTGGGCCGTAGG -5'
TT-14	5'- CGCGAATTGCGCCC -3' 3'- GCGCTTAACGCGGG -5'
(6–4)-14	5'- CGCGAA(6–4)GCGCCC -3' 3'- GCGCTTAACGCGGG -5'
CC-14	5'- CGCGAACCCGCGCCC -3' 3'- GCGCTTGGCGCGGG -5'

product formation alters both the chemical structure of the base moiety and the local tertiary structure of the duplex. The differences in the binding modes of distamycin A between the normal target sequence and the UV-damaged DNA are described.

Results

Binding of Distamycin A to Undamaged and UV-Damaged 20-Base-Pair (bp) Duplexes. To test the distamycin binding to UV-damaged DNA, 20-bp duplexes, d(CCTACGCGAATT-CGGCATCC)·d(GGATGCCGAATTCGCGTAGG), in which **TT** represents the photoproduct site, were prepared by hybridizing the chemically synthesized, damage-containing strands to the complementary oligonucleotide. Although short oligonucleotide duplexes have been used to analyze the distamycin binding by circular dichroism (CD) spectroscopy,^{26–28} we chose a relatively long sequence because the formation of the (6–4) photoproduct destabilizes the thermal stability of DNA duplexes.²⁹ The binding of distamycin A was analyzed by CD spectroscopy, using four types of duplexes (Chart 2): (1) TT-20 had the target site (AATT) for distamycin A in a G·C-rich sequence and was used as a positive control, (2) (6–4)-20 contained the (6–4) photoproduct within the target sequence in one strand of the duplex, (3) CPD-20 contained another type of UV lesion for comparison, and (4) the target sequence was disrupted in CC-20, which was used as a negative control. Titration experiments with distamycin A were carried out, and the results are shown in Figure 1. Distamycin A was able to bind to the duplex containing the (6–4) photoproduct, as indicated by the induced CD signals in the long wavelength region (Figure 1b), whereas its binding was reduced to a great extent when the duplex contained the CPD (Figure 1c) or when the two T·A base pairs in the target sequence were changed to C·G pairs (Figure 1d).

Analysis of Distamycin Binding to 14-bp Duplexes by CD Spectroscopy. In the experiments using CC-20, in which the target sequence for distamycin A was disrupted, an induced CD signal in the long wavelength region was observed, although the intensity was low (Figure 1d). We supposed that this residual signal showed nonspecific binding of distamycin to this duplex. To analyze the binding properties of distamycin in detail, we searched for shorter duplexes, which would not have the

- (10) Sugasawa, K.; Ng, J. M. Y.; Masutani, C.; Iwai, S.; van der Spek, P. J.; Eker, A. P. M.; Hanaoka, F.; Bootsma, D.; Hoeijmakers, J. H. J. *Mol. Cell* **1998**, *2*, 223–232.
- (11) Sugasawa, K.; Okamoto, T.; Shimizu, Y.; Masutani, C.; Iwai, S.; Hanaoka, F. *Genes Dev.* **2001**, *15*, 507–521.
- (12) Iwai, S.; Shimizu, M.; Kamiya, H.; Ohtsuka, E. *J. Am. Chem. Soc.* **1996**, *118*, 7642–7643.
- (13) Iwai, S.; Mizukoshi, T.; Fujiwara, Y.; Masutani, C.; Hanaoka, F.; Hayakawa, Y. *Nucleic Acids Res.* **1999**, *27*, 2299–2303.
- (14) Fujiwara, Y.; Masutani, C.; Mizukoshi, T.; Kondo, J.; Hanaoka, F.; Iwai, S. *J. Biol. Chem.* **1999**, *274*, 20027–20033.
- (15) Kim, J.-K.; Choi, B.-S. *Eur. J. Biochem.* **1995**, *228*, 849–854.
- (16) Mizukoshi, T.; Kodama, T. S.; Fujiwara, Y.; Furuno, T.; Nakanishi, M.; Iwai, S. *Nucleic Acids Res.* **2001**, *29*, 4948–4954.
- (17) Spector, T. I.; Cheatham, T. E., III; Kollman, P. A. *J. Am. Chem. Soc.* **1997**, *119*, 7095–7104.
- (18) Nichols, A. F.; Itoh, T.; Graham, J. A.; Liu, W.; Yamaizumi, M.; Linn, S. *J. Biol. Chem.* **2000**, *275*, 21422–21428.
- (19) Wemmer, D. E. *Biopolymers* **1999**, *52*, 197–211.
- (20) Neidle, S. *Nat. Prod. Rep.* **2001**, *18*, 291–309.
- (21) Parikh, S. S.; Mol, C. D.; Slupphaug, G.; Bharati, S.; Krokan, H. E.; Tainer, J. A. *EMBO J.* **1998**, *17*, 5214–5226.
- (22) Mol, C. D.; Izumi, T.; Mitra, S.; Tainer, J. A. *Nature* **2000**, *403*, 451–456.
- (23) Bruner, S. D.; Norman, D. P. G.; Verdine, G. L. *Nature* **2000**, *403*, 859–866.
- (24) Serre, L.; Pereira de Jésus, K.; Boiteux, S.; Zelwer, C.; Castaing, B. *EMBO J.* **2002**, *21*, 2854–2865.
- (25) Fromme, J. C.; Verdine, G. L. *EMBO J.* **2003**, *22*, 3461–3471.

- (26) Rentzeperis, D.; Marky, L. A. *Biochemistry* **1995**, *34*, 2937–2945.
- (27) Chen, F.-M.; Sha, F. *Biochemistry* **1998**, *37*, 11143–11151.
- (28) Lah, J.; Vesnaver, G. *Biochemistry* **2000**, *39*, 9317–9326.
- (29) Jing, Y.; Kao, J. F.; Taylor, J.-S. *Nucleic Acids Res.* **1998**, *26*, 3845–3853.

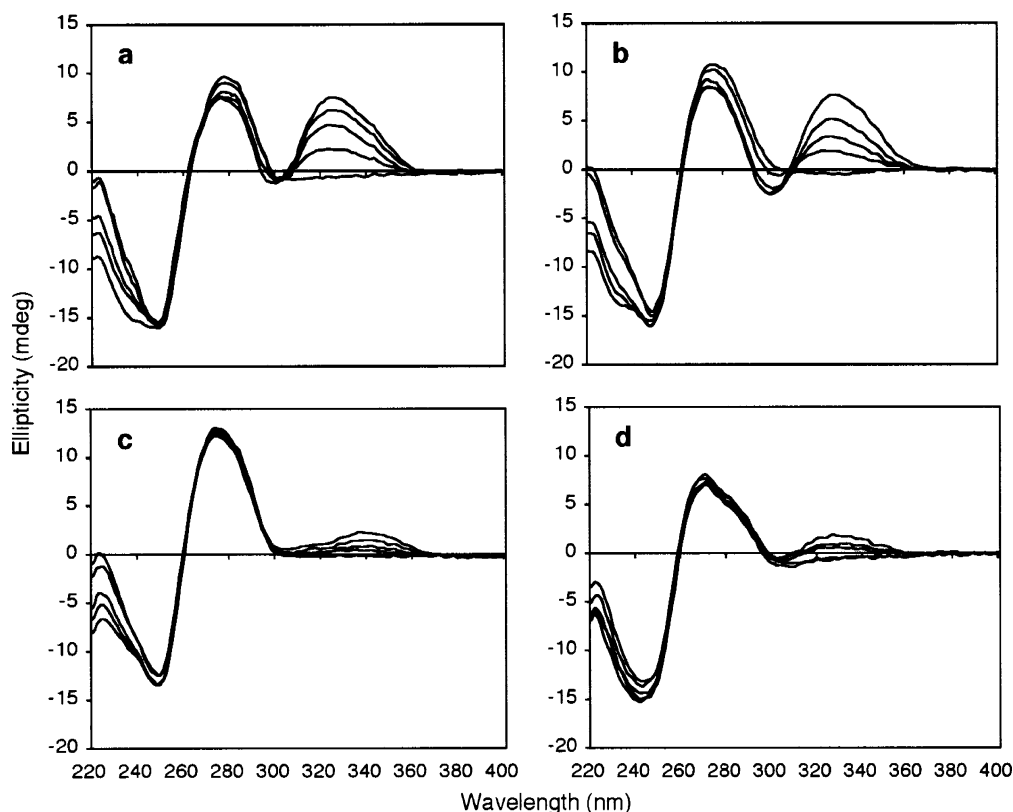


Figure 1. CD spectra of distamycin A complexed with TT-20 (a), (6-4)-20 (b), CPD-20 (c), and CC-20 (d). The samples contained 2.5 μ M duplex, 100 mM NaCl, and 10 mM sodium cacodylate (pH 7.0), and the distamycin/duplex molar ratios were 0, 0.5, 1.0, 1.5, and 2.0.

problem of nonspecific binding. We tried to prepare a 12-bp duplex containing the (6-4) photoproduct, d(CGCGAAT(6-4)TGCGC)·d(GCGCAATTCGCG), but its melting curve showed no transition, suggesting that hybridization did not occur within the tested temperature range. We then added two C·G pairs at one end of the duplex to make (6-4)-14 (Chart 2). When the solution of (6-4)-14 was heated, this duplex showed a transition from the double-strand state to the single-strand one, which started at about 20 °C. Therefore, we used this duplex, together with the undamaged 14-bp duplex (TT-14), to analyze the distamycin binding, and CD spectra were measured at 15 °C to ensure duplex formation.

The procedure was similar to the experiments using the 20-mers, and CD spectra were measured at NaCl concentrations of 100 and 500 mM. Effects of nonspecific binding are reportedly excluded at 500 mM NaCl.²⁸ Binding of distamycin A to the photoproduct-containing duplex was detected, as shown in Figure 2b. The ellipticity values at 330 nm were plotted against the distamycin/duplex ratios, as shown in Figure 3, and comparison of the plotting revealed a clear difference between TT-14 and (6-4)-14. The slope for TT-14 was steeper than that for (6-4)-14, and TT-14 reached a plateau at a lower drug concentration. Using the CD titration data, distamycin binding to each duplex was analyzed by curve fitting. In this analysis, binding of distamycin A to a single site or multiple identical, independent sites was assumed, and the data were fitted by the nonlinear least-squares method, using the equation described in the Experimental Section. The dissociation constants (K_d) and the stoichiometries (n) that gave best-fit curves shown in Figure 3 are summarized in Table 1. The affinity of distamycin

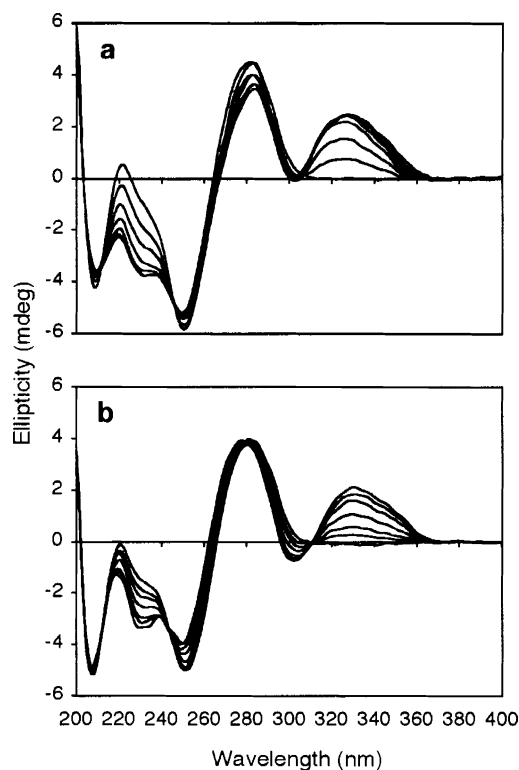


Figure 2. CD spectra of distamycin A complexed with TT-14 (a) and (6-4)-14 (b). The distamycin/duplex molar ratios were 0, 0.5, 1.0, 1.5, 2.0, 2.5, and 3.0.

A for TT-14 was somewhat higher than that for (6-4)-14, and the salt concentration hardly affected the distamycin binding to the photoproduct-containing duplex. More importantly, the

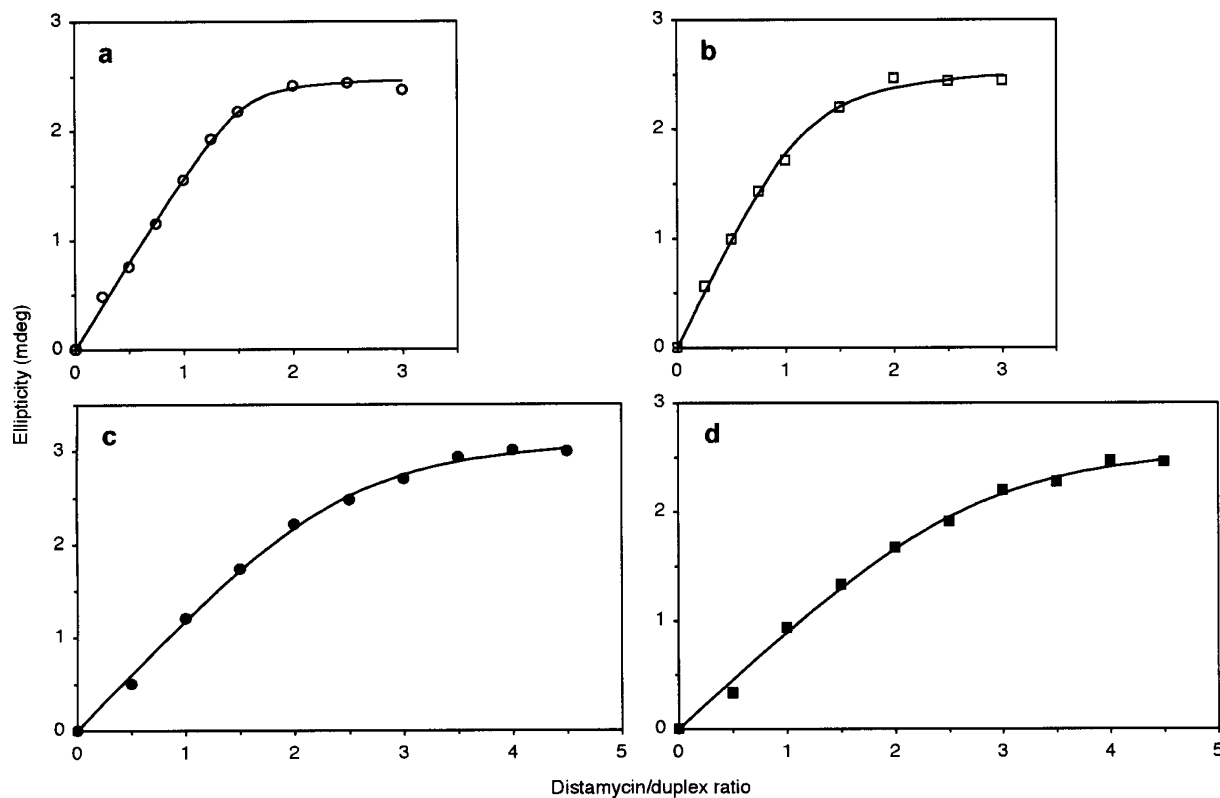


Figure 3. CD titration plots and best-fit curves for distamycin binding to TT-14 (a and b) and (6-4)-14 (c and d). CD spectra were measured in a buffer containing 100 mM (a and c) or 500 mM (b and d) NaCl, and the ellipticity values at 330 nm were plotted against the distamycin/duplex ratios.

Table 1. Distamycin A Binding Parameters Obtained from the CD Titration Curves

duplex	NaCl (mM)	K_d (M)	n (per duplex)
TT-14	100	5.9×10^{-8}	1.54
TT-14	500	2.4×10^{-7}	1.18
(6-4)-14	100	4.2×10^{-7}	2.50
(6-4)-14	500	5.4×10^{-7}	2.76

results suggested that at least two distamycin molecules bound to (6-4)-14, whereas TT-14 formed a 1:1 complex.

Analysis of Binding Modes Using CD Difference Spectra.

The CD difference spectra obtained in the titration experiments are shown in Figure 4. The spectra were not affected by the salt concentration, but their characteristics were different between TT-14 and (6-4)-14. In the spectra of TT-14, three isoelliptic points (212, 246, and 306 nm) were maintained throughout the titration. The positive intensity enhancement at 255 nm was weak, and the direction of the progressive intensity increase of the band around 278 nm changed from negative to positive at the distamycin/duplex ratio of 1.5, as shown in the insets in Figure 4. In the case of (6-4)-14, four isoelliptic points (213, 242, 280, and 310 nm) were observed, and a large positive CD band was induced near 260 nm upon the distamycin binding.

Melting Curves of the Complexes. In the measurement of UV absorption spectra, it was found that the absorbance at wavelengths longer than 310 nm was increased upon complex formation. We thought that this property could be used to monitor the dissociation of distamycin, so we measured the melting curves of the complexes between the duplexes (TT-14 and (6-4)-14) and distamycin A. Two types of mixtures, in which the molar ratios of distamycin A and the duplex were 1:1 and 2:1, were used for comparison. The melting curve of a

1:1 mixture of CC-14, in which the target site was disrupted, was also measured, and the obtained result was used to exclude the nonspecific binding effect in the melting curve of the 2:1 mixture of TT-14. As shown in Figure 5, all of the curves for TT-14 and (6-4)-14 showed a single transition, and the important point is that the decrease in the absorption of the 2:1 mixture of the distamycin-(6-4)-14 complex was about twice as large as that observed for the 1:1 mixture (Figure 5b), whereas there was only a small difference in the TT-14 case (Figure 5a).

Discussion

In this study, we have found that distamycin A, a natural antibiotic that is known as a minor groove binder, can bind to DNA duplexes containing the (6-4) photoproduct at its target site. We tested the distamycin binding based on rational reasoning derived from our DNA recognition studies of the UV-DDB protein, but still we are rather surprised that the expected binding was observed. Distamycin A recognizes its target site by van der Waals contacts and hydrogen bonds. In particular, the hydrogen-bonding interactions were studied thoroughly by NMR spectroscopy³⁰⁻³² and X-ray crystallography.³³⁻³⁵ NMR studies revealed that a single distamycin molecule bound to the

- (30) Pelton, J. G.; Wemmer, D. E. *Biochemistry* **1988**, *27*, 8088-8096.
 (31) Pelton, J. G.; Wemmer, D. E. *Proc. Natl. Acad. Sci. U.S.A.* **1989**, *86*, 5723-5727.
 (32) Pelton, J. G.; Wemmer, D. E. *J. Am. Chem. Soc.* **1990**, *112*, 1393-1399.
 (33) Coll, M.; Frederick, C. A.; Wang, A. H.-J.; Rich, A. *Proc. Natl. Acad. Sci. U.S.A.* **1987**, *84*, 8385-8389.
 (34) Chen, X.; Ramakrishnan, B.; Rao, S. T.; Sundaralingam, M. *Nat. Struct. Biol.* **1994**, *1*, 169-175.
 (35) Chen, X.; Ramakrishnan, B.; Sundaralingam, M. *J. Mol. Biol.* **1997**, *267*, 1157-1170.

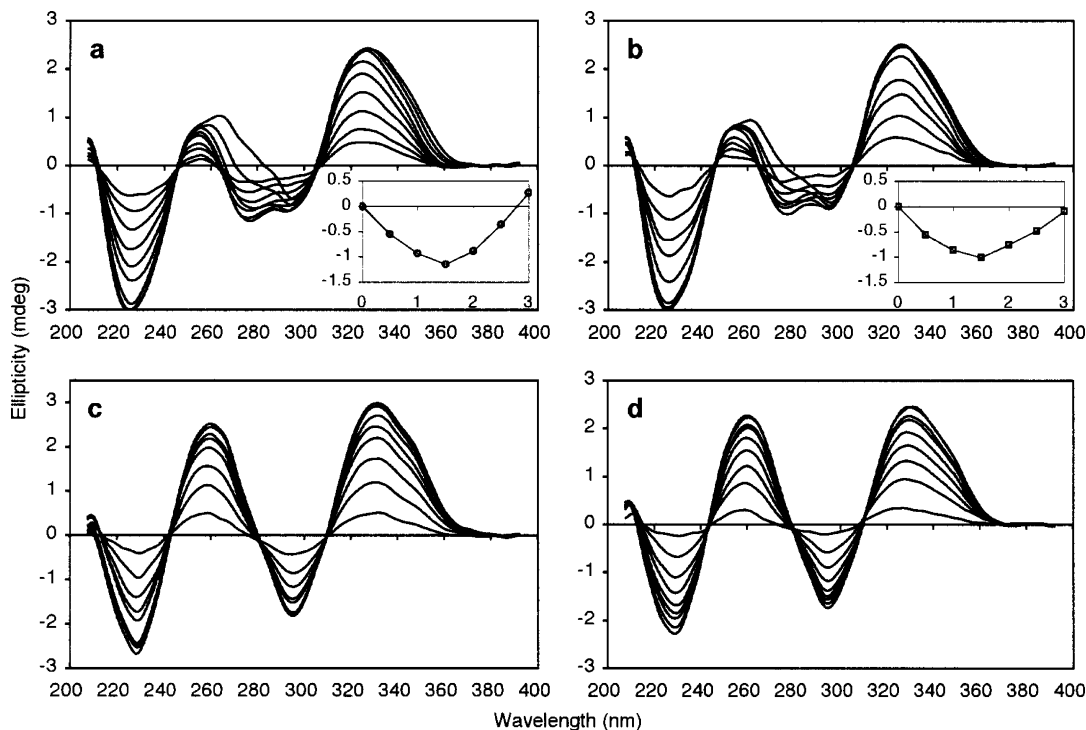


Figure 4. Induced CD difference spectra of distamycin A complexed with TT-14 (a and b) and (6-4)-14 (c and d) at 100 mM (a and c) and 500 mM (b and d) NaCl. The distamycin/duplex molar ratios were 0, 0.25, 0.5, 0.75, 1.0, 1.25, 1.5, 2.0, 2.5, and 3.0 (a and b) and 0, 0.5, 1.0, 1.5, 2.0, 2.5, 3.0, 3.5, 4.0, and 4.5 (c and d). The insets are 278 nm ellipticity versus distamycin/duplex ratio plots.

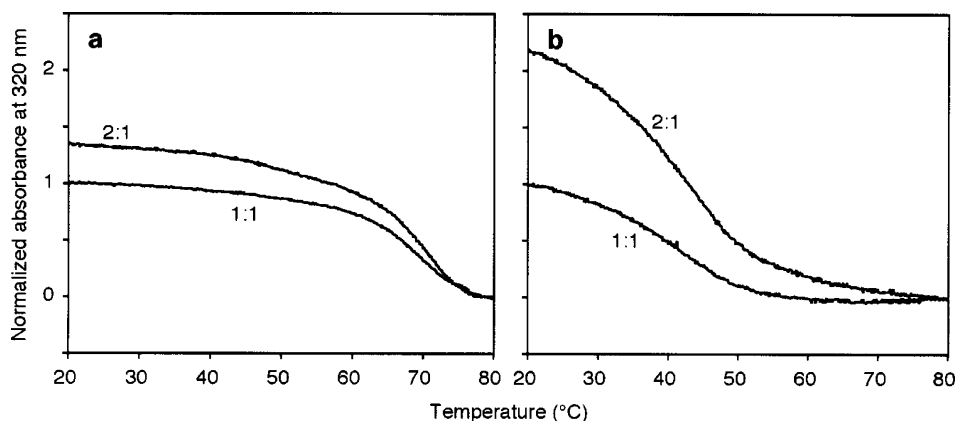


Figure 5. Normalized melting curves of the 1:1 and 2:1 mixtures between distamycin A and the duplex (TT-14, a; (6-4)-14, b) measured at 320 nm.

target site of AATT·AATT,³⁰ while the addition of one or two A·T pairs, which makes the target sequence AAATT or AAATTT, resulted in the formation of a complex containing two distamycin molecules in a side-by-side manner.^{31,32} We used the former target sequence, in which all of the O2 atoms reportedly form hydrogen bonds with distamycin.³⁰ When one of the TT sites is changed into the (6-4) photoproduct, the chemical structure of the base moiety is altered, and, although both of the O2 atoms exist after photoproduct formation, their spatial positions are also affected because the 5'-pyrimidine and 3'-pyrimidone rings of the (6-4) photoproduct are linked perpendicularly.^{36,37} As shown in our previous study, a local conformational change of the DNA helix also occurs upon photoproduct formation.¹⁶

Distamycin A binding was tested by CD spectroscopy, a standard method for the detection of its specific binding,²⁶⁻²⁸ using the 20-bp duplexes. It was clearly shown that this compound could bind to a duplex containing the (6-4) photoproduct (Figure 1). It should be noted that specific binding did not occur with the duplex containing the CPD (Chart 1b, Figure 1c), another type of UV damage that seems to cause smaller distortions in DNA than the (6-4) photoproduct.

Binding of distamycin A was investigated in detail by using the 14-bp duplexes. Titration experiments by CD spectroscopy were carried out (Figure 2), and the results were analyzed by curve fitting (Figure 3 and Table 1). For the duplex containing the target sequence (TT-14), the K_d and n values and the salt effect were similar to those reported previously.^{27,28} Distamycin A bound to the photoproduct-containing duplex ((6-4)-14) with a K_d value in the submicromolar range, irrespective of salt

(36) Rycyna, R. E.; Alderfer, J. L. *Nucleic Acids Res.* **1985**, *13*, 5949-5963.
 (37) Taylor, J.-S.; Garrett, D. S.; Wang, M. J. *Biopolymers* **1988**, *27*, 1571-1593.

concentrations. The obtained n value suggested that at least two distamycin molecules bound to this duplex.

The binding modes can also be discussed using the induced CD difference spectra. Chen and Sha reported that 1:1 and 2:1 drug–duplex complexes could be distinguished using CD spectral characteristics.²⁷ Complex formation between TT-14 and distamycin A induced a weak positive intensity enhancement at 255 nm, and an isoelliptic point at 264 nm was lost at high drug concentrations (Figure 4a and b). These characteristics indicate the 1:1 binding mode. In contrast, difference spectra for (6–4)-14 showed a large positive CD band induced near 260 nm and maintenance of an isoelliptic point at 280 nm (Figure 4c and d), which are typical of the 2:1 drug–duplex complex. The difference spectra obtained for TT-14 at the highest distamycin concentration may indicate the 2:1 binding because they are similar to those observed for (6–4)-14 and are slightly affected by the salt concentration. The maintenance of all of the isoelliptic points in Figure 4c and d demonstrates that the 2:1 complex is formed even at low distamycin concentrations.

We observed that the absorbance at wavelengths longer than 310 nm changed upon complex formation and thought that the stoichiometry could be confirmed by using this property. The melting curves, that is, the temperature dependence of the absorption, of the distamycin–DNA complexes were measured at 320 nm, as shown in Figure 5. The T_m values, that is, the transition midpoints, of the TT-14 and (6–4)-14 complexes were about 70 and 42 °C, respectively, while the T_m of (6–4)-14 without distamycin, measured at 260 nm, was 37.6 °C. It is reasonable that complex formation stabilized the duplex, and the complex with the undamaged duplex was more stable than that with the photoproduct-containing duplex, as expected from the K_d values determined from the CD titration data. More importantly, the decrease in the absorbance of the 2:1 mixture was about twice as large as that of the 1:1 mixture in the case of (6–4)-14 (Figure 5b), whereas only a small difference was observed for TT-14 (Figure 5a). Because this decrease indicates the amount of distamycin bound to each duplex, this result supports the 2:1 stoichiometry for the (6–4) photoproduct-containing duplex. The single transition observed for the 2:1 mixture of (6–4)-14 suggests that a 1:1 complex was not formed as an intermediate during the dissociation.

From the titration experiments by CD spectroscopy and the measurement of the melting curves, it is concluded that a 2:1 distamycin–DNA complex, which is similar to that observed for a 5-bp target site,³¹ is formed at the (6–4) photoproduct. Previously, it was discussed that the width of the minor groove was important for the recognition of distamycin A,²⁷ and we showed that formation of the (6–4) photoproduct caused a local unwinding of a DNA duplex.¹⁶ This unwinding may well change the geometry and/or the flexibility of the minor groove to accommodate two distamycin molecules.

In this study, we have shown that distamycin A can bind to DNA duplexes containing the (6–4) photoproduct. The stoichiometry change demonstrated in this study suggests that the distamycin A recognition mechanism is different between the normal target and the photoproduct site. Further studies for the elucidation of the recognition mechanism will enable us to design compounds that specifically bind to UV-damaged DNA.

Experimental Section

Materials. The building blocks of the (6–4) photoproduct¹² and the CPD³⁸ were synthesized as described previously. Oligonucleotides were synthesized on an Applied Biosystems model 394 DNA synthesizer (Applied Biosystems, Foster City, CA), using the nucleoside phosphoramidites for the ultramild DNA synthesis (Glen Research, Sterling, VA). Phenoxyacetic anhydride was used as a capping agent. The oligonucleotides were deprotected with ammonium hydroxide at room temperature for 2 h and were purified by HPLC, using a μ Bondasphere C18 5 μ m 300 Å column (3.9 \times 150 mm, Waters, Milford, MA) with a linear gradient of acetonitrile in 0.1 M triethylammonium acetate (pH 7.0). The obtained oligonucleotides were quantified using the optical method reported previously.³⁹ The duplexes shown in Chart 2 were prepared by heating the mixtures of the two strands (5 nmol) in water (50 μ L) at 80 °C for 3 min and cooling them gradually to room temperature. The melting curves of the 12-bp and 14-bp duplexes containing the (6–4) photoproduct were measured at 260 nm, in 10 mM sodium phosphate buffer (pH 7.0) containing 100 mM NaCl, on a Beckman DU-7000 spectrophotometer (Beckman Coulter Inc., Fullerton, CA). Distamycin A was purchased from Sigma (St. Louis, MO).

CD Spectroscopy. The CD spectra of the distamycin–20-bp DNA complexes were measured on an Aviv model 62 DS/202 spectrophotometer (Aviv Associates, Lakewood, NJ). The sample solutions (400 μ L) contained 2.5 μ M each duplex, 100 mM NaCl, and 10 mM sodium cacodylate (pH 7.0), and titrations were conducted by adding 0.9 μ L aliquots of a distamycin solution to increase the distamycin/duplex molar ratio by 0.5. The CD spectra of the distamycin-14-bp DNA complexes were measured at 15 °C on a JASCO J-805 spectrophotometer (JASCO Corp., Tokyo, Japan). The sample solutions (600 μ L) contained 2.5 μ M of each duplex, 100 or 500 mM NaCl, and 10 mM sodium phosphate (pH 7.0), and titrations were conducted in a similar manner.

Curve Fitting. If a DNA duplex D contains n identical, independent binding sites for a ligand L, the number of the ligand bound per DNA is written as

$$\nu = \frac{n[L]/K_d}{1 + [L]/K_d} \quad (1)$$

where K_d and $[L]$ are the dissociation constant for each binding site and the concentration of the free ligand, respectively.⁴⁰

For the equilibrium,

$$\nu = \frac{[L]_t - [L]}{[D]_t} \quad (2)$$

where $[L]_t$ and $[D]_t$ are the total concentrations of the ligand and the DNA duplex, respectively.

From eqs 1 and 2,

$$[L] = \frac{([L]_t - K_d - n[D]_t) + \sqrt{([L]_t - K_d - n[D]_t)^2 + 4K_d[L]_t}}{2} \quad (3)$$

Consequently, the concentration of the bound form of the ligand is written as

- (38) Murata, T.; Iwai, S.; Ohtsuka, E. *Nucleic Acids Res.* **1990**, *18*, 7279–7286.
 (39) Borer, P. N. In *Handbook of Biochemistry and Molecular Biology*, 3rd ed.; *Nucleic Acids*; Fasman, G. D., Ed.; CRC Press: Cleveland, 1975; Vol. 1, p 589.
 (40) Cantor, C. R.; Schimmel, P. R. In *Biophysical Chemistry Part III: The Behavior of Biological Macromolecules*; W. H. Freeman and Company: New York, 1980; p 855.

$$[L]_t - [L] = \frac{([L]_t + K_d + n[D]_t) - \sqrt{([L]_t - K_d - n[D]_t)^2 + 4K_d[L]_t}}{2} \quad (4)$$

At the wavelength λ , which is well outside the UV absorption region of the DNA, the observed CD signal intensity at each data point $\theta_{\text{obs}}(\lambda)$ is expressed as

$$\begin{aligned} \theta_{\text{obs}}(\lambda) &= \theta_{\text{sat}}(\lambda) \frac{[L]_t - [L]}{n[D]_t} \\ &= \frac{\theta_{\text{sat}}(\lambda)}{n[D]_t} \frac{([L]_t + K_d + n[D]_t) - \sqrt{([L]_t - K_d - n[D]_t)^2 + 4K_d[L]_t}}{2} \end{aligned} \quad (5)$$

where $\theta_{\text{sat}}(\lambda)$ is the CD signal intensity of the sample when the binding sites are fully occupied by the ligand. The CD titration data at 330 nm were analyzed by the nonlinear least-squares fitting method using eq 5 to estimate $\theta_{\text{sat}}(330 \text{ nm})$, K_d , and n .

Measurements of the Melting Curves of the Complexes. The samples contained TT-14, (6-4)-14, or CC-14 (4.25 μM) and distamycin A (4.25 or 8.50 μM) in a buffer (120 μL) containing 100 mM NaCl and 10 mM sodium phosphate (pH 7.0). Melting curves were measured at 320 nm on a Shimadzu UV-1700 spectrophotometer equipped with a TMSPC-8 temperature controller. The temperature was raised from 10 to 80 $^{\circ}\text{C}$, and the absorbance data were collected at intervals of 0.1 $^{\circ}\text{C}$. To exclude the nonspecific binding effect in the 2:1 mixture of TT-14, the melting curve obtained for the 1:1 mixture of CC-14 was subtracted from the TT-14 2:1 curve.

Acknowledgment. We thank Mr. Toshiro Nagai and Dr. Keiji Hirose (Osaka University) for help in measuring CD spectra, and Dr. Yoshiyuki Tanaka (Tohoku University) and Dr. Masayuki Takahashi (CNRS & Universite de Nantes) for helpful discussions. This study was supported in part by a Grant-in-Aid for Scientific Research from the Ministry of Education, Culture, Sports, Science, and Technology, Japan.

JA048851K